Facile nitric acid activation of carob seeds for efficient recovery of heavy metals from water

M. Farnane[a], A. Machrouhi[a], M. Khnifira[a], M. Barour[a], R. Elmoubarki[a], M. Abdennouri[a], H. Tounsadi[b], S. Qourzal[c], N. Barka[a],*

[a]Sultan Moulay Slimane University of Beni Mellal, Research Group in Environmental Sciences and Applied Materials (SEMA), FP Khouribga, B.P. 145, 25000 Khouribga, Morocco, Tel. +212 661 66 66 22; Fax: +212 523 49 03 54;
emails: barkanoureddine@yahoo.fr (N. Barka), Farnane.meryem@gmail.com (M. Farnane),
machrouhi.aicha90@gmail.com (A. Machrouhi), khnifiramalak2014@gmail.com (M. Khnifira), barourmohammed1@gmail.com (M. Barour),
elmoubarkirachid@gmail.com (R. Elmoubarki), abdennourimohamed@yahoo.fr (M. Abdennouri)
[b]Laboratoire d'Ingénierie, d'Electrochimie, de Modélisation et d'Environnement (LIEME), Université Sidi Mohamed Ben Abdellah,
Faculté des Sciences Dhar El Mahraz, Fès, Morocco, email: hananetounsadi@gmail.com (H. Tounsadi)
[c]Equipe de Catalyse et Environnement, Département de Chimie, Faculté des Sciences, Université Ibn Zohr, B.P. 8106 Cité Dakhla,
Agadir, Morocco, email: samir_qourzal@yahoo.fr (S. Qourzal)

ABSTRACT

In order to prepare an efficient activated carbon, facile chemical activation of carob seeds using nitric acid was investigated. Box–Behnken design coupled with response surface methodology was used to optimize the preparation conditions process for efficient sorption of cadmium and cobalt ions. The effect of various factors including impregnation ratio, activation time and activation temperature was studied extensively. The obtained activated carbons were evaluated through iodine number, methylene blue index and by their sorption capacities of cadmium and cobalt ions. Experimental results showed that the activation temperature and impregnation ratio were the most significant influencing factors. For the iodine number, the greater value of 1,034.83 mg/g was obtained for a carbon-impregnated with 0.05 g/g and activated at 500°C for 1 h 30 min. While the maximum value of the methylene blue index was 279.59 mg/g, it was acquired for activated carbon with an impregnation ratio of 0.075 g/g, activated at 500°C for 2 h. In the case of the elimination of the heavy metal ions, the carbon activated at 500°C during 2 h with an impregnation ratio of 0.025 g/g has a higher sorption capacity for cadmium ions. While, in the same conditions but for 1 h, the maximum sorption of cobalt was obtained. The highest sorption capacities via the Langmuir isotherm model were 91.92 mg/g for cadmium and 79.18 mg/g for cobalt, respectively. Structural properties and surface chemistry of the optimized activated carbons were studied by X-ray diffraction, Fourier-transform infrared spectroscopy, scanning electron microscopy, Boehm titration and pHpzc. The obtained activated carbon-based carob seeds would be one of the potential adsorbents for heavy metal ions removal.

Keywords: Carob seeds; Nitric acid activation; Heavy metals; Box–Behnken design

* Corresponding author.

1. Introduction

In aquatic ecosystems, cadmium and cobalt are considered highly toxic heavy metals. They possess the ability to concentrate along the food chain and to accumulate in certain organs of the human body. Therefore, the elimination of these species from various industrial effluents is essential to reduce their effect before releasing in the environment. Many methods and techniques of depollution were evaluated during the last years. Among these techniques, we can cite the chemical precipitation processes [1], ultrafiltration [2], ion exchange [3], solvent extraction [4], electrochemical treatment [5] and adsorption [6]. This latter can be considered as an efficient and economical method for the removal of heavy metals at different concentrations. The principle of adsorption treatment is to trap the ions of heavy metals by a solid material called adsorbent. Among the most using adsorbents, activated carbons are the most effective due to their highly porous structure, their large surface area and their greater sorption capacity.

In recent years, several less expensive and renewable precursors have been used for the production of activated carbon such as carob shells [7], *Thapsia transtagana stems* [8], almond shell and orange peel [9], *Theobroma cacao pod husk* [10], *Citrullus colocynthis* peel [11], marine red alga *Pterocladia capillacea* [12], *Diplotaxis harra* [13], sawdust [14], coffee-shell [15], mung bean husk [16], date palm tree [17], chestnut oak shells [18] and sea mango [19].

For the preparation of activated carbons, there are two main types of activation methods: physical activation and chemical activation. The physical method, also commonly known as the gas activation method. In the physical activation process, the carbonized raw materials are activated at a high temperature of 1,073–1,273 K with water vapor [20], flue gas (a mixture with water vapor, CO_2, N_2, etc.) [21], or air and other activated gases to form a developed microporous carbon material. Then, the chemical activation method includes the addition of chemicals into the raw material or chars, after the heating under the protection of inert gas to yield activated products. Chemical activation is widely applied due to its lower activation temperature, its shorter activation time, its higher product yield, and its greater specific surface area as compared to the physical process. At present, the well-known chemical agents used are $ZnCl_2$, H_3PO_4, H_2SO_4, K_2S, KCNS, HNO_3, H_2O_2, $KMnO_4$, $(NH_4)_2S_2O_8$, NaOH, KOH and K_2CO_3 for the production of activated carbons with a high surface area and appropriate porous structure [22–26]. In the chemical activation process, the preparation of activated carbon depends on many factors including the impregnation ratio, the activation temperature, the activation time and other factors. Afterward, in order to optimize such studies, the experimental design is a quick and cost-effective method applied to understand and optimize any manufacturing processes [7,8,27].

The present work explored the use of carob seeds as a potential feedstock for activated carbon preparation by nitric acid activation. The influences of impregnation ratio, activation temperature and activation time on the performance of activated carbon (AC) were investigated by Box–Behnken experimental design. Four responses were analyzed, which are; iodine number (IN), methylene blue index (MB index), cadmium Cd(II) and cobalt Co(II) ions removal. The ACs produced at the optimal conditions were characterized by the Fourier-transform infrared spectroscopy (FTIR), scanning electron microscopy (SEM), X-ray diffraction (XRD), Boehm titration and the point of zero charge (pH_{PZC}). Equilibrium data for metal ions sorption was tested by Langmuir and Freundlich isotherm models.

2. Materials and methods

2.1. Materials

All the chemicals used in this study were of analytical grade, $Cd(NO_3)_2 \cdot 4H_2O$ (98%), $Co(NO_3)_2 \cdot 6H_2O$ (98%), NaCl (99.5%), iodine (I_2) (100%), sodium thiosulfate ($Na_2S_2O_3 \cdot 5H_2O$) (99%), Na_2CO_3 (99%), $NaHCO_3$ (99%) and HCl (37%) were purchased from Sigma-Aldrich (Germany). HNO_3 (65%) was provided by Sharlau (Spain). NaOH (99.5%) from Merck (Germany). Potassium iodide (KI) was obtained from Pharmac (Morocco) and methylene blue was purchased from Panreac (Spain).

2.2. Preparation of activated carbons

The carob seeds were collected from the region of Khenifra in Morocco. Firstly, they were crushed and sieved to the desired particle sizes (1–2 mm). The powder was impregnated with nitric acid at an impregnation ratio of (g HNO_3/g carbon) of 0.025, 0.050 or 0.075 at 50 mL of distilled water during 6 h. After, the samples were heated at 105°C for 24 h to remove excess moisture. Then, the impregnated products were thermally activated in a furnace at 400°C, 500°C or 600°C during desired activation times (1 h, 1 h 30 or 2 h) under a flow of N_2 gas. The residual nitric acid was eliminated from the activated carbons by washing with hot deionized water until neutral pH. The obtained powder was then dried at 105°C until constant weight, powdered using a domestic mixer and sieved in particles of size lower than 125 μm using a normalized sieve. Finally, the resulting powder was kept in a hermetic bottle for further tests. The activated carbon yield after the carbonization process was estimated by 10%.

2.3. Characterization of activated carbons

2.3.1. Iodine number

Iodine number was measured according to the ASTM D4607-94 method; 1 g of each AC was boiled for 30 s with 10.0 mL of 5% HCl solution and subsequently cooled. About 100 mL of 0.1 N iodine solution was added to the mixture and stirred for 30 min. The resulting solution was filtered and 50 mL of the filtrate was titrated with 0.1 N sodium thiosulfate using starch as an indicator.

The iodine number was calculated using the following equation:

$$\text{I.Iode}\left(\frac{mg}{g}\right) = \left\{ \begin{array}{l} \left(N_1 \times 126.93 \times N_1\right) - \left[\dfrac{V_1 + V_{HCl}}{V_f}\right] \times \\ \left(N_{Na_2S_2O_3} \times 126.93\right) \times V_{Na_2S_2O_3} \end{array} \right\} / M_C \qquad (1)$$

where N_1 is the normality of the iodine solution; V_1 is the volume of iodine added; V_{HCl} is the volume of HCL (5%) added; V_f is the filtered volume used in the titration; $N_{Na_2S_2O_3}$ is the normality of the solution of sodium thiosulfate; $V_{Na_2S_2O_3}$ is the volume of sodium thiosulfate poured and M_C is the mass of activated carbon.

2.3.2. Methylene blue index

The methylene blue index is a measure of mesoporosity (2–5 nm) present in activated carbon. It is defined as the maximum amount of dye adsorbed on 1.0 g of adsorbent. In order to have maximum sorption capacities of methylene blue onto ACs, the adsorption isotherms were investigated. A stock solution of methylene blue was prepared by dissolving the desired weight of MB dye in distilled water. Sorption experiments were investigated in a series of beakers containing 100 mL of MB solution by adding 100 mg of each AC. Sorption equilibrium was established for different methylene blue initial concentrations between 20 and 500 mg/L for 12 h at room temperature. After each sorption experiment, samples were centrifuged at 3,400 rpm for 10 min and dilution has been made to have a final concentration in the region of calibration. Then, residual concentrations were determined using the spectrophotometric method at the wavelength of maximum absorbance of 665 nm.

2.3.3. Heavy metal ions removal

Firstly, metal ions solutions of cadmium or cobalt ions were prepared by dissolving the desired weight of $Cd(NO_3)_2 \cdot 4H_2O$ or $Co(NO_3)_2 \cdot 6H_2O$ in distilled water. Then, subsequent solutions at desired concentrations were prepared by dilution. Adsorption experiments were established in a series of beakers containing 50 mL of the metal ion solution at 100 mg/L and 50 mg of activated carbon sample. The mixtures were stirred for 3 h at 500 rpm. The pH of solutions was adjusted at 6.50 during the experiment with either 0.1 M of HCl or NaOH and measured by a sensION+ PH31 pH meter. After each sorption experiment, samples were centrifuged at 3,400 rpm for 10 min and the metal ion concentrations were determined using a Perkin-Elmer atomic absorption spectrophotometer (AAnalyst 200).

The adsorption capacity at equilibrium was defined as the amount of adsorbate per gram of adsorbent (in mg/g) and was calculated using the following equation:

$$q = \frac{(C_0 - C)}{R} \tag{2}$$

where q is the adsorbed quantity (mg/g), C_0 is the initial dye concentration (mg/L), C is the residual heavy metal ion concentration (mg/L), and R is the mass of activated carbon per liter of aqueous solution (g/L).

Sorption equilibrium for optimized activated carbons was investigated for different metals through an initial concentration between 20 and 200 mg/L. The experimental results were correlated to Langmuir and Freundlich isotherm models via non-linear fitting using Origin 6.0 software.

2.3.4. Surface chemistry

Functional groups of activated carbons were examined by FTIR using a Scotch-SP1 spectrophotometer. The samples are packaged in the form of pellets, consisting of 0.5–2 mg of the activated carbon, diluted in 100 mg of KBr. The results are presented in transmittance for wavenumbers between 4,000 and 500 cm⁻¹. Basic and oxygenated acidic surface groups were quantified by Boehm titrations [28]. The pH point of zero charge (pH$_{PZC}$) was determined by the pH drift according to the method proposed by Noh and Schwarz [29]. The morphological characteristics of the prepared activated carbon were analyzed by SEM using a FEI Quanta 200 model. A small amount of each sample was finely powdered and mounted directly onto an aluminum sample holder using a two-sided adhesive carbon model. Crystallographic characterization of the activated carbons was examined by XRD measurements. The XRD patterns were recorded at room temperature using a Bruker-axis D2-phaser advance diffractometer equipped with a copper anticathode (CuKα line, λ = 1.5406 Å) operating at 30 kV and 10 mA. The samples were irradiated in a 2θ angular range varying from 10° to 80°, with a measurement step of 0.01° and counting time in steps of 0.5 s/step.

2.4. Experimental design

In the present study, the three-level three factorial Box–Behnken experimental designs with 17 experiments were applied to optimize the preparation conditions and heavy metals removal efficiency of activated carbons. The factor levels were coded as −1 (low), 0 (central point) and 1 (high). Table 1 shows the Box–Behnken design levels for the experimental parameters used: impregnation ratio (X_1), activation time (X_2) and activation temperature (X_3). The Design Expert 8.0.7.1 Trial software was used for generating the statistical experimental design and analyzing the observed data. A manual regression method was used to fit the second-order polynomial equation (Eq. (3)) to the experimental data and to recognize the relevant model terms. Considering all the linear terms, square terms and by linear interaction items, the quadratic response model can be described as:

$$Y = b_0 + b_1X_1 + b_2X_2 + b_3X_3 + b_{12}X_1X_2 + b_{13}X_1X_3 + b_{23}X_2X_3 + b_{11}X_1^2 + b_{22}X_2^2 + b_{33}X_3^2 \tag{3}$$

where Y is the responses of interest (iodine number (Y_1), methylene blue index (Y_2), the adsorption capacity of Cd(II) (Y_3) and adsorption capacity of Co(II) (Y_4)).

Table 1
Process factors and their levels

Factors		Levels		
		−1	0	+1
X_1	Impregnation ratio (g/g)	0.025	0.050	0.075
X_2	Activation time (h)	1	1.50	2
X_3	Activation temperature (°C)	400	500	600

3. Results and discussion

3.1. Optimization of preparation conditions

3.1.1. Experimental results

The experimental matrix of factors in coded and actual values and results for the four responses studied are shown in Table 2. From this table, it could be seen that the activation temperature and the impregnation ratio have a significant effect on the development of the iodine number. The maximum iodine number value of 1,034.83 mg/g was obtained for an activated carbon impregnated with a ratio of 0.05 g/g and activated for 1 h 30 min at a temperature of 500°C. Furthermore, the methylene blue index varies between 79.11 and 279.59 mg/g. The higher mesoporosity was obtained for the activated carbon impregnated with a ratio of 0.075 g/g and activated at 500°C for 2 h. The maximum adsorption efficiency of cadmium was 50.05 mg/g for activated carbon impregnated with a ratio of 0.025 g/g and activated for 2 h at a temperature of 500°C. The activated carbon impregnated with a ratio of 0.025 g/g and activated for 1 h at a temperature of 500°C gives the highest cobalt adsorption capacity of 43.51 mg/g.

In addition, the regression analysis was performed to fit the response functions with the experimental data. The values of the regression coefficient obtained are presented in Table 3. The impregnation ratio has a positive effect on the iodine number, the methylene blue index and a negative effect on the elimination of heavy metal ions. However, the activation time has a positive effect on the methylene blue index, on the elimination of cadmium and a negative effect on the iodine number and on the removal of cobalt. While the activation temperature had a negative effect on the four responses. In addition, the analysis of interaction effects indicates significant interactions on the four responses with negative or positive effects. The significant interactions are on the iodine number, one between the impregnation ratio and the activation temperature (b_{13} = 73.31) with a positive effect and another one significant interaction between activation temperature and activation temperature with a negative effect (b_{33} = –224.80).

3.1.2. Analysis of variance

Analysis of variances (ANOVA) was used to determine the significant effects and interactions on the four responses at a confidence level of 95%. The data for the coded quadratic models are presented in Tables 4a–d. The results showed that the equations adequately represented the actual relationship between each response and the

Table 3
Values of model coefficients for the four responses

Main coefficients	Y_1	Y_2	Y_3	Y_4
b_0	1,011.29	216.61	38.65	24.77
b_1	87.78	34.14	–4.23	–2.12
b_2	–12.57	8.93	5.22	–1.60
b_3	–153.94	–60.41	–13.99	–9.01
b_{12}	–14.87	33.43	–5.92	–0.11
b_{13}	73.31	–19.02	–3.36	–0.57
b_{23}	–30.58	–14.52	–2.11	–4.45
b_{11}	–76.56	–18.56	2.94	5.66
b_{22}	–12.30	8.04	–5.05	5.00
b_{33}	–224.80	–60.82	–5.85	–12.34

Table 2
Factorial experimental design matrix coded, real values and experimental results of the four responses

Run	Coded values			Actual values			Responses (mg/g)			
	A	B	C	A	B	C	IN	MB index	Cd(II)	Co(II)
1	–1	0	–1	0.025	1h30	400	863.10	153.68	45.07	25.19
2	0	0	0	0.050	1h30	500	1,034.83	228.84	36.12	27.48
3	1	–1	0	0.075	1h00	500	974.79	187.84	32.14	32.06
4	0	–1	–1	0.050	1h00	400	835.17	208.06	34.13	20.61
5	–1	–1	0	0.025	1h00	500	849.13	192.49	30.15	43.51
6	1	0	–1	0.075	1h30	400	960.82	237.52	49.05	27.48
7	0	0	–1	0.050	1h30	400	932.90	171.04	43.58	22.90
8	0	1	0	0.050	2h00	500	918.94	212.24	46.07	22.14
9	–1	1	0	0.025	2h00	500	891.02	147.02	50.05	38.17
10	0	1	1	0.050	2h00	600	611.77	104.89	15.22	5.34
11	1	1	0	0.075	2h00	500	1,002.71	279.59	29.15	30.53
12	–1	0	1	0.025	1h30	600	304.60	79.11	24.68	11.45
13	0	1	–1	0.050	2h00	400	904.90	265.40	45.57	31.30
14	0	0	1	0.050	1h30	600	653.66	104.08	12.74	6.11
15	0	–1	1	0.050	1h00	600	765.36	91.49	14.73	13.74
16	0	–1	0	0.050	1h00	500	1,030.64	239.94	22.69	33.59
17	1	0	1	0.075	1h30	600	695.55	86.88	15.22	11.45

significant variables. The *F*-value implies that the models are significant and values of "Prob. > *F*" less than 0.05 indicates that model terms are significant. Especially larger *F*-value with the associated *P*-value (smaller than 0.05. confidence interval) means that the experimental systems can be modeled effectively with less error. Consequently, the effects considered as significant model terms can be used to optimize the experimental system.

3.1.2.1. Iodine number

According to the ANOVA analysis for the iodine number (Table 4a), the significant effects are impregnation ratio (X_1), activation time (X_2), activation temperature (X_3) and the interactions X_1X_3, X_2X_3, X_1^2, X_3^2 (Eq. (4)). The impregnation ratio and the interaction between the impregnation ratio and the activation temperature have a positive effect on the iodine number. While other factors and interactions have a negative effect. Therefore, the increase in the impregnation ratio increases the iodine number resulted

in an increase in the microporosity of activated carbons. On the other hand, the increase of the activation time and the activation temperature reduces the number of iodine.

$$Y_1 = 998.99 + 90.75X_1 - 13.75X_2 - 153.94X_3 + 73.31X_1X_3 - 30.58X_2X_3 - 74.10X_1^2 - 219.86X_3^2 \qquad (4)$$

3.1.2.2. Methylene blue index

According to the ANOVA analysis (Table 4b), the main effects influencing the methylene blue index are the impregnation ratio (X_1), the activation time (X_2), the activation temperature (X_3) and the interactions X_1X_2, X_1X_3, X_3^2 (Eq. (5)). The impregnation ratio, the activation time and the interaction between the impregnation ratio and the activation time have a positive effect on the methylene blue index response. However, the activation temperature and the interactions between the impregnation ratio and the activation temperature and between the activation temperature and the activation temperature have a negative

Table 4a
Analysis of variance of iodine number

Source	Sum of squares	Degree of freedom	Mean square	*F*-value	*p*-value Prob. > *F*	
Model	502,592.97	7	71,799.00	12.18	0.001	
X_1	65,887.95	1	65,887.95	11.18	0.009	
X_2	1,981.40	1	1,981.40	0.34	0.576	
X_3	209,458.61	1	209,458.61	35.55	0.0002	
X_1X_3	21,495.96	1	21,495.96	3.65	0.088	
X_2X_3	4,098.44	1	4,098.44	0.70	0.426	Significant
X_1^2	22,499.58	1	22,499.58	3.82	0.082	
X_3^2	190,450.68	1	190,450.68	32.32	0.0003	
Residual	53,031.81	9	5,892.42			
Corr. total	555,624.78	16				

$R^2 = 0.9068$; $R^2_{aju} = 0.7870$

Table 4b
Analysis of variance of methylene blue index

Source	Sum of squares	Degree of freedom	Mean square	*F*-value	*p*-value Prob. > *F*	
Model	61,877.73	6	10,312.96	16.29	0.0001	
X_1	8,679.42	1	8,679.42	13.71	0.004	
X_2	1,157.11	1	1,157.11	1.83	0.206	
X_3	32,404.56	1	32,404.56	51.20	3.09E-05	
X_1X_2	4,828.44	1	4,828.44	7.63	0.020	Significant
X_1X_3	1,446.66	1	1,446.66	2.29	0.162	
X_3^2	1,4848.95	1	14,848.95	23.46	0.001	
Residual	6,329.10	10	632.91			
Corr. total	68,206.83	16				

$R^2 = 0.9471$; $R^2_{aju} = 0.8791$

Table 4c
Analysis of variance of removal of cadmium

Source	Sum of squares	Degree of freedom	Mean square	F-value	p-value Prob. > F	
Model	2,511.20	7	358.74	16.33	0.0002	
X_1	133.45	1	133.45	6.08	0.036	
X_2	272.70	1	272.70	12.42	0.006	
X_3	1,817.37	1	1,817.37	82.741	7.83E-06	
X_1X_2	151.42	1	151.42	6.89	0.028	
X_1X_3	45.16	1	45.16	2.06	0.185	Significant
X_2^2	95.32	1	95.32	4.34	0.067	
X_3^2	149.66	1	149.66	6.81	0.028	
Residual	197.68	9	21.96			
Corr. total	2,708.88	16				

$R^2 = 0.9464$; $R_{aju}^2 = 0.8776$

Table 4d
Analysis of variance of removal of cobalt

Source	Sum of squares	Degree of freedom	Mean square	F-value	p-value Prob. > F	
Model	1,779.65	7	254.24	12.47	0.001	
X_1	35.28	1	35.28	1.73	0.221	
X_2	13.19	1	13.19	0.65	0.442	
X_3	717.14	1	717.14	35.17	0.0002	
X_1X_3	1.31	1	1.31	0.06	0.806	
X_2X_3	86.91	1	86.91	4.26	0.069	Significant
X_1^2	88.90	1	88.90	4.36	0.066	
X_3^2	810.95	1	810.95	39.77	0.0001	
Residual	183.52	9	20.39			
Corr. total	1,963.17	16				

$R^2 = 0.9323$; $R_{aju}^2 = 0.8453$

effect. As a result, the methylene blue index increases when the impregnation ratio, the activation time and the interaction between the impregnation ratio and the activation time increase. Therefore, the increase of the MB index induces the increase of the activated carbons mesoporosity.

$$Y_2 = 231.17 + 34.14X_1 + 10.49X_2 - 56.93X_3 + 33.34X_1X_2 - 19.02X_1X_3 - 60.44X_3^2 \tag{5}$$

3.1.2.3. Removal of cadmium

For the cadmium removal response (Table 4c), the most important factors are the impregnation ratio (X_1), the activation time (X_2), the activation temperature (X_3) and the interactions X_1X_2, X_1X_3 and X_3^2 (Eq. (6)). The activation time has a positive effect on the removal of cadmium ion. On the other hand, other factors and interactions indicate a negative effect. Moreover, the removal of cadmium decreased when the impregnation ratio, activation temperature and X_1X_2, X_1X_3, X_2^2 and X_3^2 interactions varied from lower

to higher levels. Therefore, if the activation time is at the high level (2 h), the removal of cadmium increased.

$$Y_3 = 41.31 - 4.23X_1 + 5.22X_2 - 13.48X_3 - 5.92X_1X_2 - 3.36X_1X_3 - 6.61X_2^2 - 6.78X_3^2 \tag{6}$$

3.1.2.4. Removal of cobalt

Based on Table 4d, the most significant effects for the removal of cobalt are the impregnation ratio (X_1), the activation time (X_2), the activation temperature (X_3) and the interactions X_1X_3, X_2X_3, X_1^2 and X_3^2 (Eq. (7)). While, the impregnation ratio, the activation time and the activation temperature and the X_1X_3, X_2X_3 and X_3^2 interactions had a negative impact on the removal of cobalt ions. However, the interaction between the impregnation ratio and the impregnation ratio has a positive effect. In other words. The adsorption of cobalt increases if the impregnation ratio, the activation time and the activation temperature

and the interactions between 'the impregnation ratio and the activation temperature', between 'the activation time and the activation temperature' and between 'the activation temperature and the activation temperature' are in their low levels.

$$Y_4 = 29.77 - 2.10X_1 - 1.12X_2 - 9.01X_3 - 0.57X_1X_3 - 4.45X_2X_3 + 4.66X_1^2 - 14.35X_3^2 \quad (7)$$

3.1.3. Response surface analysis

Three-dimensional (3D) response surface plots of the predictive quadratic model for the significant interactions are shown in Figs. 1–4. For the iodine number and cobalt removal, the most important interactions are activation temperature/impregnation ratio and activation temperature/activation time. For the methylene blue index and cadmium removal, the most significant interactions

are activation time/impregnation ratio and activation temperature/impregnation ratio.

3.1.3.1. Iodine number

From Fig. 1a, it could be seen that the iodine number increase with decreasing the activation temperature regardless of the impregnation ratio. The maximum iodine number was observed at an activation temperature of 400°C with an activation time of 2 h. Fig. 1b indicates that the iodine number increases if the activation temperature decreases whatever the activation time. For that, the maximum iodine number was obtained at an activation temperature of 400°C and an impregnation ratio of 0.075 g/g.

3.1.3.2. Methylene blue index

It can be seen from Fig. 2a that the increase of activation time and impregnation ratio provokes an increment
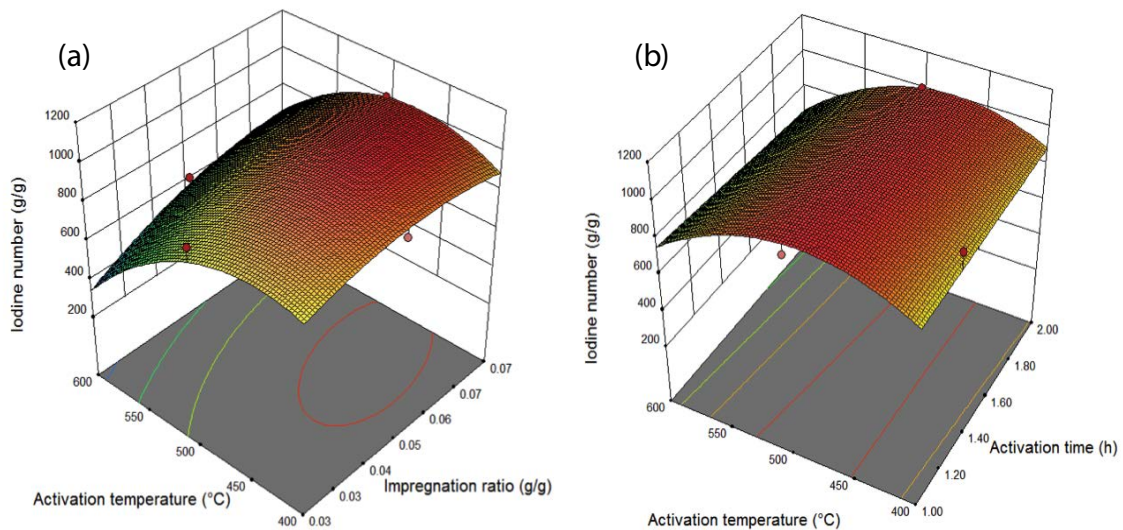
Fig. 1. Surface response plot for the iodine number.
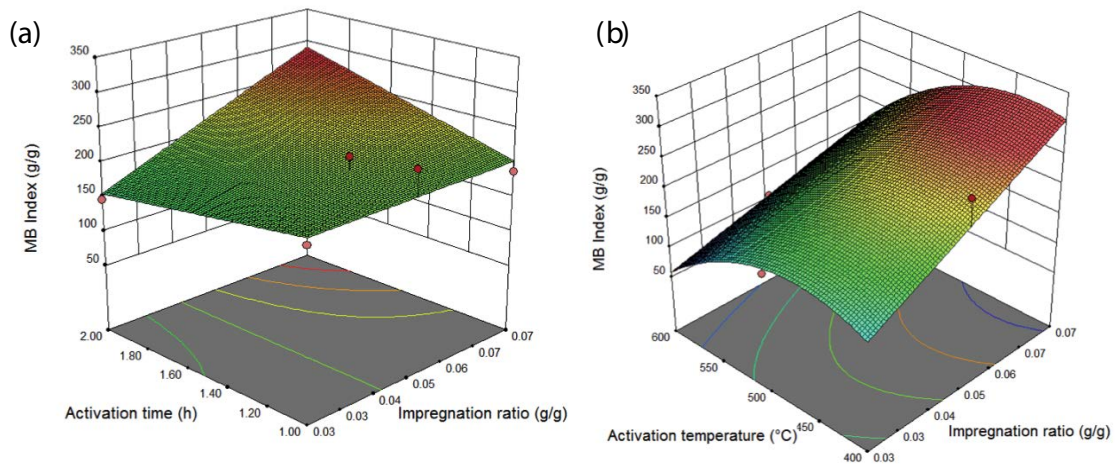
Fig. 2. Surface response plot for the index of methylene blue.
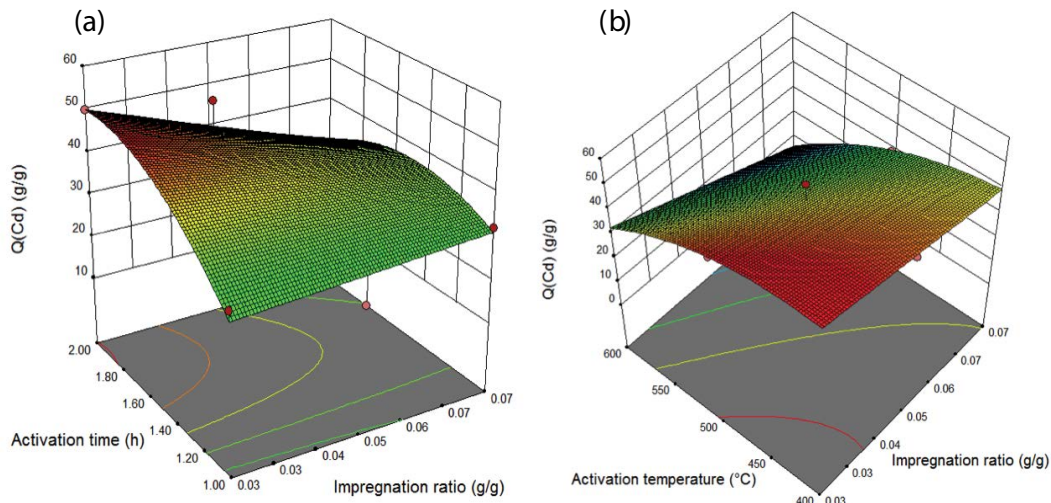
Fig. 3. Surface response plot for the removal of cadmium.
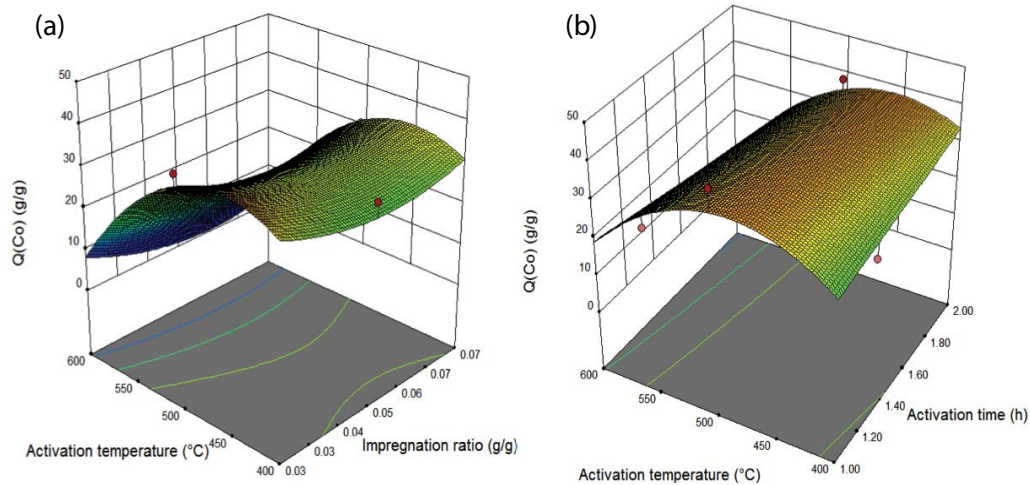
Fig. 4. Surface response plot for the removal of cobalt.

in methylene blue index. The maximum methylene blue index was observed at an activation time of 2 h and an impregnation ratio of 0.075 g/g when the activation temperature is set at 500°C. Moreover, Fig. 2b indicates that the methylene blue index increases when the activation temperature decreases and the impregnation ratio increases. The maximum value of the methylene blue index was obtained with an impregnation ratio of 0.075 g/g and activation at 400°C for 2 h.

3.1.3.3. Cadmium ions removal

The adsorption of cadmium increases with the increasing activation time and the decreasing of impregnation ratio as can be seen from Fig. 3a. Cadmium removal has acquired the maximum at an activation temperature of 500°C for 2 h with an impregnation ratio of 0.025 g/g. Also, the cadmium removal increased at the higher activation time and lower impregnation ratio (Fig. 3b). Maximum capacity of cadmium removal is obtained at an activation

temperature of 400°C, an impregnation ratio of 0.025 g/g and an activation time of 2 h.

3.1.3.4. Cobalt ions removal

Fig. 4a indicates that the removal of cobalt increases with the decrease of the activation temperature and the impregnation ratio. The maximum response is obtained at an activation temperature of 400°C when the impregnation ratio increases during 2 h. Also, Fig. 4b shows that the removal of cobalt increases with increasing activation temperature at any activation time. The maximum removal of the cobalt is observed at 500°C with an impregnation ratio of 0.025 g/g during 2 h.

3.1.4. Normal probability plot of residuals

The normal residual probability curves for the iodine number, methylene blue index, cadmium and cobalt ions removal are shown in Fig. 5. We can see from the figure that
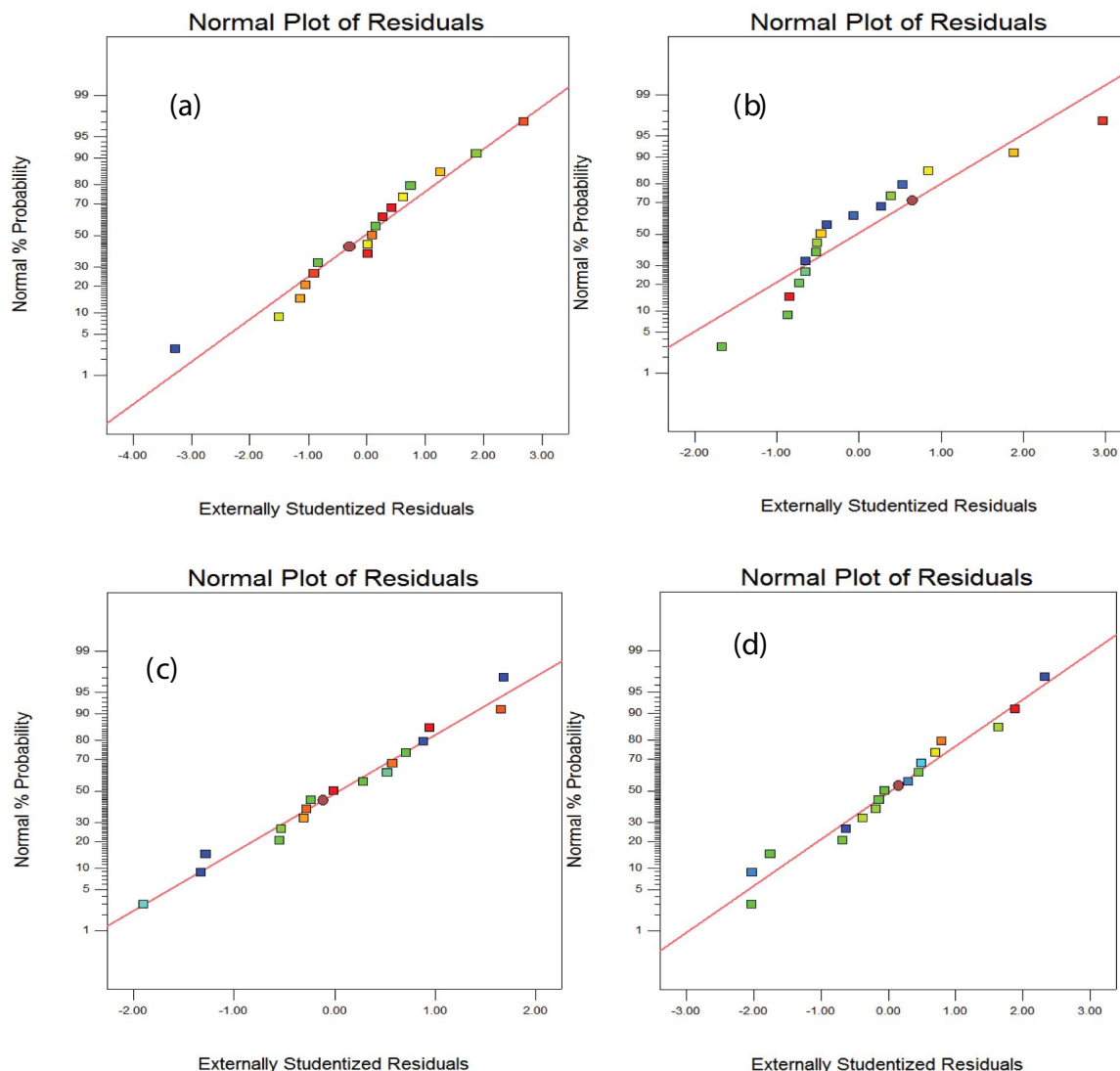
Fig. 5. Normal probability plots of residuals for the four responses: (a) iodine number, (b) MB index, (c) Cd(II) and (d) Co(II) removal capacities.

for the four studying responses, the data points are close enough to the straight line, which shows that the experiments are at the origin of a normally distributed population [30].

3.1.5. Optimization

The desirability function was used to optimize the four responses including iodine number, methylene blue index and the removal of cadmium and cobalt ions. The maximum value of the desirability function (1.000) is obtained at an activation temperature of 500°C, an activation time of 2 h and an impregnation ratio equal to 0.025 g/g. Under these optimum conditions, predicted points for iodine number, methylene blue index, sorption of Cd(II) and Co(II) were 998.99 ± 76.76 mg/g, 213.17 ± 25.16 mg/g, 41.31 ± 4.69 mg/g and 29.77 ± 4.52 mg/g respectively. Then, in order to obtain the maximum adsorption capacities, adsorption tests must be carried out under the optimum conditions.

For instance, after this statistical experimental approach using the Box–Behnken experimental design coupled with the surface of response, the optimized activated carbons have been determined. Therefore, the structural, textural properties and the chemical surface of these efficiently activated carbons were investigated. This can lead to identifying the specific characteristics of achieved activated carbons through the cadmium and cobalt sorption process.

3.2. Characterization of activated carbons

3.2.1. Fourier-transform infrared spectroscopy

The FTIR spectra of activated carbons are presented in Fig. 6. The figure shows a band at about 3,435 cm^{-1} attributed to (O–H) vibrations of hydroxyl groups for alcohols or phenols. The band at 2,132 cm^{-1} is ascribed to (C=C) vibrations of alkyne groups. The band at 1,736 cm^{-1} is attributed to carbonyl (C=O) groups. The olefinic (C=C) absorption band
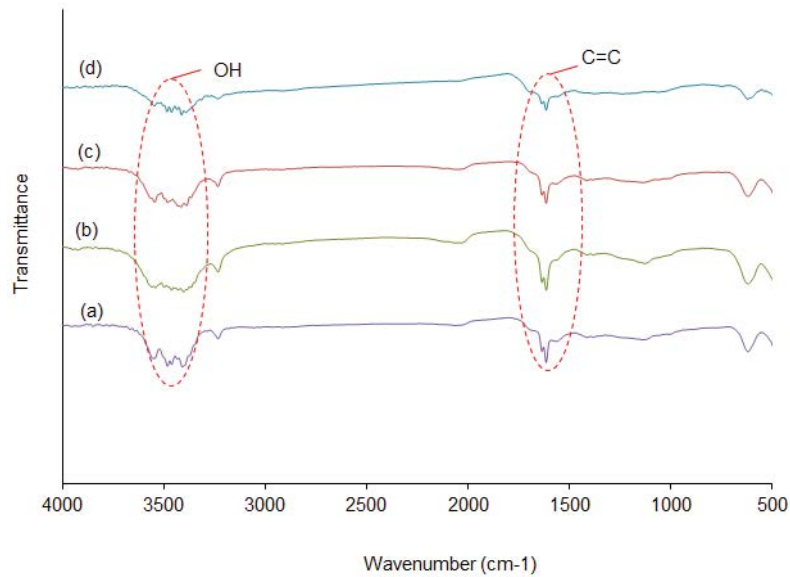
Fig. 6. FTIR spectra of activated carbons (a) 0.025 g/g-2 h-500°C, (b) 0.075 g/g-1 h-500°C, (c) 0.025 g/g-1 h-500°C and (d) 0.05 g/g-1 h-500°C.

appeared at 1,643 cm^{-1}, while the skeletal C=C vibrations in aromatic rings caused the two bands at 1,505 and 1,428 cm^{-1}. The appearance of bands between 1,300 and 900 cm^{-1} could be assigned to C–O stretching vibrations. The band caused by O–H out-of-plane bending vibrations band is located at 580 cm^{-1}.

3.2.2. Boehm titration and pH$_{pzc}$

The types and amounts of functional groups present in activated carbons were determined by the Boehm titration method which provides qualitative and quantitative information on the surface charge and hence the adsorption capacity of the activated carbons. From Table 5, it can be seen that the surface of the activated carbons consists mainly of acid groups than basic groups, indicating that the obtained activated carbons have an acidic character. It was observed that the concentrations of carboxylic and phenolic groups are higher than those of lactonic groups. Table 5 shows also the pH$_{pzc}$ values of the activated carbons. All the samples displayed values in low acidic to the neutral domain in accordance with the Boehm titration. This result suggests higher cation exchange properties for cadmium and cobalt ions.

3.2.3. SEM observation

The SEM micrographs of four ACs produced under different conditions are presented in Figs. 7a–d. The figure indicates that the ACs exhibits heterogeneous surface structures with irregular pores, which may depend on preparation conditions. Figs. 7a and c corresponding to ACs obtained under the optimal conditions show cracks, crevices, and some grains in various sizes in large holes. Therefore, it can be concluded that this activated carbon present an adequate morphological profile to adsorb metal ions. The activated carbon samples are shown in Figs. 7b and d indicate numerous cavities significantly damaged [31]. These cavities created further active sites.

3.2.4. XRD patterns of the activated carbons

The XRD patterns of the activated carbons are shown in Fig. 8. The figure shows an amorphous structure for the four samples, which is an advantageous property for well-defined porous adsorbents. The diffractograms have similar profiles; a peak at 25° and another one at 43°. These peaks are thus attributed respectively to carbon graphite reflections (002) and (100) and dehydrated hemicellulose. The highest intensity of the peak at 2θ equal to 25° results from the parallel layer stacking of the graphite turbostratic structure and the peak at 2θ of order 43° is attributed to the regular structure in the different segments of the plane. For the four samples, no obvious change of (002) diffraction peak can be shown from the XRD spectrums, but the peak around 2θ = 43° slightly decreases. The smaller microcrystalline can increase the number of unsaturated carbon atoms on the edges and corners of the sample surface, leading to the enhancement of sample surface reactivity and adsorption performance. Besides, according to the Bragg equation, the formation of interlamellar pores between layers of crystallite (100) can be enhanced by the incremental interlamellar space.

3.3. Adsorption isotherms

The equilibrium relationships between adsorbent and adsorbate are best explained by sorption isotherms. After the optimization of the preparation conditions, the activated carbons having a greater ability for the removal of cadmium and cobalt ions are AC$_1$; impregnated at 0.025 g/g and activated at 500°C during 2 h and AC$_2$; impregnated at 0.025 g/g and activated at during 1 h. Fig. 9 shows that the equilibrium sorption increased with a rise in equilibrium concentration. This augmentation was due to a higher driving force for mass transfer at high concentrations in solution. Furthermore, the AC$_1$ has a greater sorption efficiency for cadmium and AC$_2$ presents a higher sorption efficiency for cobalt. The equilibrium data were analyzed

Table 5
Chemical groups on the surface and pH$_{pzc}$ of the adsorbents

Activated carbon	Carboxylic groups (meq/g)	Lactonic groups (meq/g)	Phenolic groups (meq/g)	Total acid groups (meq/g)	Total basic groups (meq/g)	pH$_{pzc}$
0.025 g/g-2 h-500°C	0.4700	0.4420	0.4630	1.3750	0.3990	6.73
0.075 g/g-1 h-500°C	0.4720	0.4420	0.4640	1.3780	0.4030	6.62
0.025 g/g-1 h-500°C	0.4550	0.4640	0.4820	1.4010	0.4330	6.23
0.050 g/g-1 h-500°C	0.4580	0.4470	0.4550	1.3600	0.4540	6.35
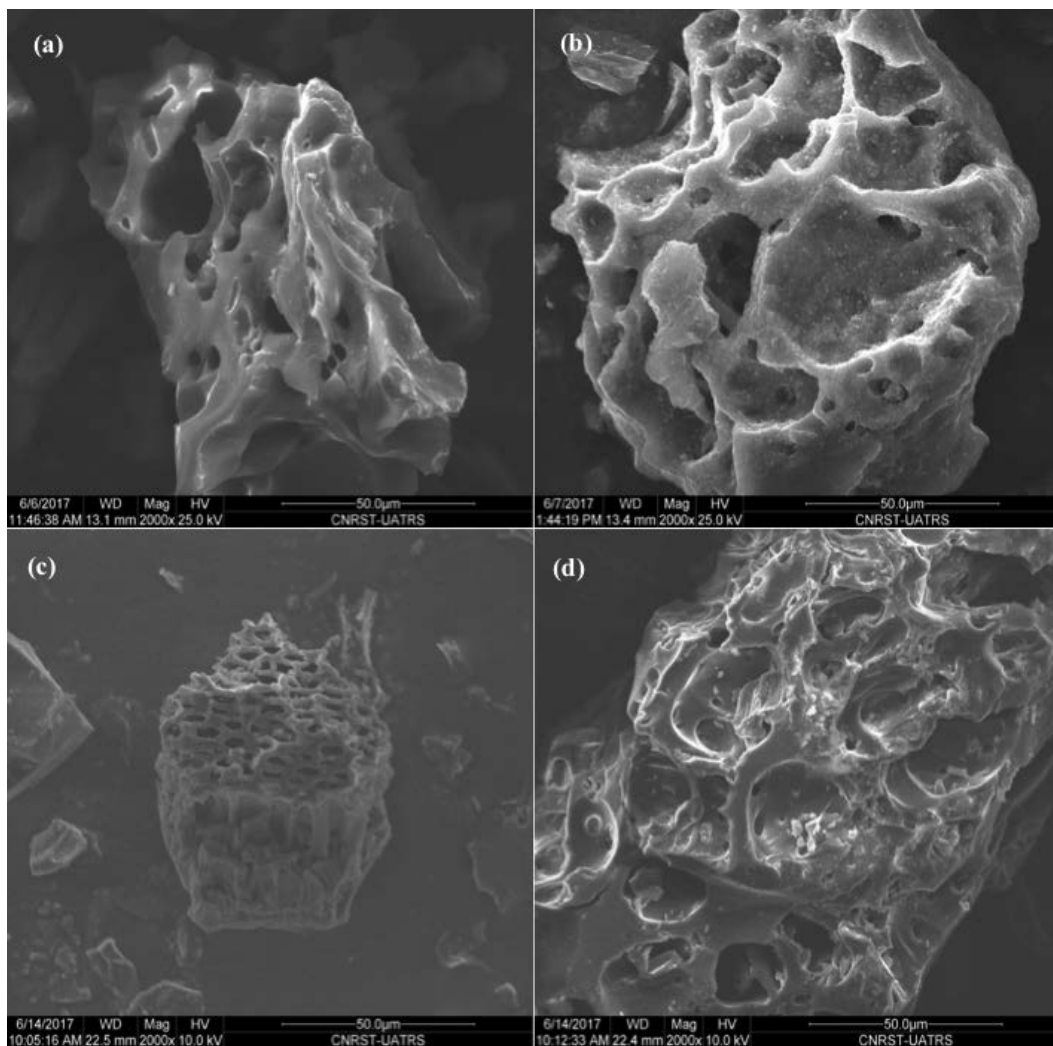
Fig. 7. SEM micrographs of activated carbon (a) 0.025 g/g-2 h-500°C, (b) 0.075 g/g-1 h-500°C, (c) 0.025 g/g-1 h-500°C and (d) 0.05 g/g-1 h-500°C.

by the well-known Langmuir and Freundlich isotherm models. These isotherms are useful for estimating the total amount of adsorbent needed to adsorb a required amount of adsorbate from the solution.

The Langmuir model presumes monolayer adsorption onto a surface containing a finite number of adsorption sites [32]. The linear form of Langmuir isotherm is represented as follows:

$$q_e = \frac{q_m K_L C_e}{1 + K_L C_e} \tag{8}$$

where q_m (mg/g) is the maximum monolayer biosorption capacity and K_L (L/mg) is the Langmuir equilibrium constant related to the adsorption affinity. C_e is the equilibrium concentration.
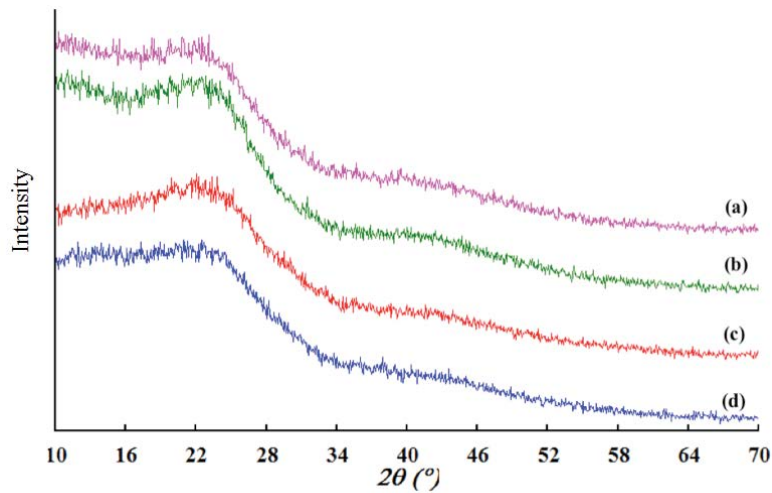
Fig. 8. XRD patterns of activated carbon (a) 0.025 g/g-2 h-500°C, (b) 0.075 g/g-1 h-500°C, (c) 0.025 g/g-1 h-500°C and (d) 0.05 g/g-1 h-500°C.
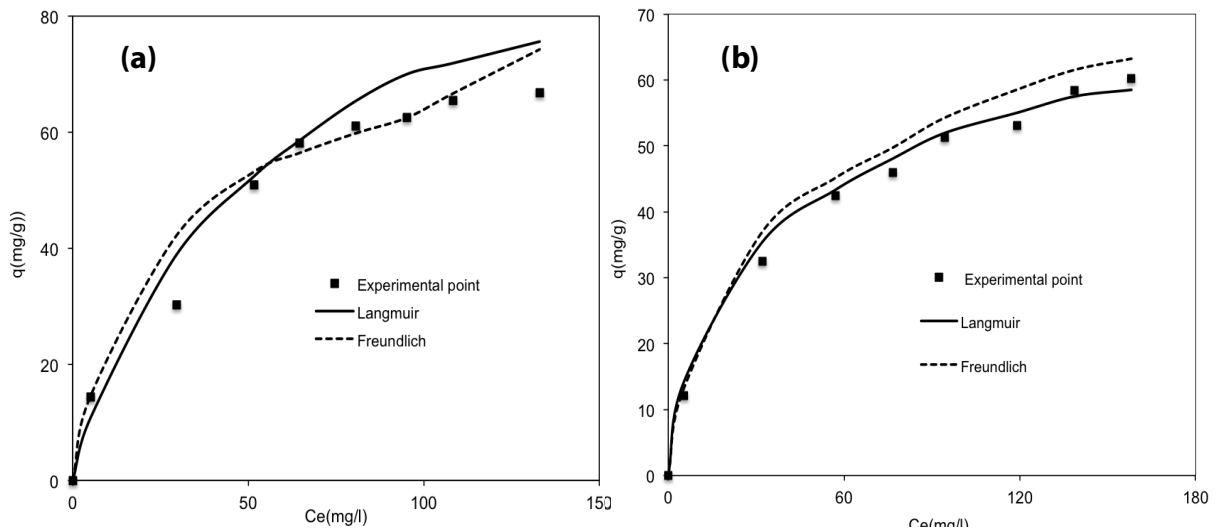
Fig. 9. Experimental points and nonlinear fitted curves isotherms of ACs (a) Cd(II) onto 0.025 g/g-2 h-500°C and (b) Co(II) onto 0.025 g/g-1 h-500°C.

The Freundlich isotherm is an empirical model of heterogeneous surface sorption with non-uniform distribution of heat sorption and affinities [33]. The form of the Freundlich equation can be stated as follows:

$$q_e = K_F \, C_e^{1/n} \tag{9}$$

where K_F (mg$^{1-1/n}$/g/L$_n$) is the Freundlich constant and n is the heterogeneity factor. The K_F value is related to the adsorption capacity; while $1/n$ value is related to the adsorption intensity or surface heterogeneity ranges between 0 and 1. When $1/n$ is close to zero, the surface becomes more heterogeneous. If $1/n$ is within 0.1 and 1, the adsorption process is good, but as the $1/n$ constant is closer to 1, heterogeneity of the adsorbent surface is less important. A constant close to 0.1 shows the importance of heterogeneity [34].

Table 6 indicates that the Langmuir model described better experimental data. The n value for the Freundlich model is greater than 1, indicating a favorable adsorption process. The adsorption capacities obtained by the Langmuir model are 91.92 mg/g for cadmium sorption, obtained by the activated carbon impregnated to 0.025 g/g during 2 h with an activation temperature of 500°C, and 79.18 mg/g for cobalt sorption obtained by the activated carbon impregnated to 0.025 g/g during 1 h with an activation temperature of 500°C, respectively.

The maximum Langmuir adsorption capacities mentioned above were compared with other active carbons studied in the literature (Table 7). It may be found that the assumed optimum activated carbons have higher adsorptive efficiencies than the majority of active carbons used for the adsorption of cadmium and cobalt.

4. Mechanism sorption process

The performance quality of prepared activated carbons has been examined via different analysis including iodine

number, MB index and heavy metals sorption using statistical experimental design. While the purpose of this work was investigated according to the sorption process. The substances adsorbates are already classified on two different types which are organic compounds and heavy metal ions. In this regard, the MB dye was studied via the MB index and the heavy metal ions are presented by cadmium and cobalt ions. In general, the adsorption capacity and affinity of these materials are determined by structural and textural physical properties and by surface chemical nature of activated carbons.

According to the temperature range during activation of carob seeds, oxygen on the carbon surface was presented in two types of surface groups: one was presented as carboxyl and lactones evolved on degassing as CO_2 and is acidic in nature. The other oxygen group is quinones, evolved by degassing as CO and is nonacidic in nature [42]. The amounts of these two types of groups depend on the raw material and the steps of the preparation of activated carbons. Therefore, the activated carbon still as being an amphoteric material due to the existence of both negatively and positively charged sites on its surface. When activated carbon is placed in an aqueous solution, the type of sites dominate depends on the solution of pH. In aqueous solution, the

acidic surface of oxygen groups under ionization produced H^+ ions, the degree of ionization depended on the pH solution. The formation of surface functional groups determines the surface charge for electrostatic interactions and reactive sites for chemical interactions between the activated carbon surface and the studying toxically substances. It could be seen that the sorption of cationic species depends on the acid oxygen-containing surface functional groups; However, the removal of non-ionic or anionic adsorbate compounds was closely correlated to the surface basicity and oxygen-free Lewis basic sites [43].

In fact, the sorption of heavy metal ions and organic compounds is considered to take a trade-off relationship concerning the surface acidity as an example of MB which is a cationic dye. It was also widely recognized that organic molecules sorption onto activated carbon has been done through the interaction between the functional groups including carboxylic, phenolic and lactonic groups situated at the activated carbon surface and the groups of organic molecules. Also, this sorption may be established via hydrogen bonding and/or electron donor–acceptor mechanism [44]. The adsorption mechanism of heavy metals ions onto activated carbon was switched from ion exchange with the acidic functional groups to the cationic metal ions

Table 6
Isotherm parameters for the sorption of Cd(II) and Co(II) of AC-0.025g/g-2h-500°C and AC-0.025 g/g-1 h-500°C

Isotherms	Parameters	0.025 g/g-2 h-500°C Cd(II)	0.025 g/g-1 h-500°C Co(II)
Langmuir	q_m (mg/g)	91.92	79.18
	K_L (L/mg)	0.02	0.02
	R^2	0.99	0.99
	N	3.79	2.85
Freundlich	K_F (mg$^{1-1/n}$ g/L$_n$)	18.79	10.22
	R^2	0.99	0.99

Table 7
Sorption capacities (mg/g) for activated carbons

Activated carbon	Activating agent	Cd(II)	Co(II)	References
Activated carbon bagasse	$ZnCl_2$	38.03	–	[35]
Activated carbon *Phragmites australis*	H_3PO_4	40.42	–	[36]
Activated carbon *Phragmites australis*	$(NH_3)_3PO_4$	58.33	–	[36]
Activated carbon *Phragmites australis*	$(NH_3)_2HPO_4$	46.42	–	[36]
Activated carbon sweet lime peels (303 K)	$ZnCl_2$	105.13	–	[37]
Activated carbon sweet lime peels (313 K)	$ZnCl_2$	107.67	–	[37]
Activated carbon sweet lime peels (323 K)	$ZnCl_2$	110.99	–	[37]
Activated carbon oxalate–treated	$K_2C_2O_4$	–	50.76	[38]
Activated carbon *Thespesia populnea* bark	H_2SO_4	–	22.72	[39]
Activated *Glebionis coronaria* L.	KOH	115.99	46.80	[40]
Activated *Glebionis coronaria* L.	H_3PO_4	118.78	82.55	[41]
Activated *Diplotaxis harra*	H_3PO_4	51.83	69.86	[13]
Activated carob shell	KOH	90.58	77.24	[7]
Activated carob seeds (0.025g/g-2h-500°C)	HNO_3	91.92	–	This study
Activated carob seeds (0.025g/g-1h-500°C)	HNO_3	–	79.18	This study

interaction. This result evolved the higher cation exchange properties for cadmium and cobalt ions and for cationic organic molecules (MB).

On other hand, the prepared activated carbons were positively charged below the point of zero charge (pHpzc) and negatively charged above it. At pH ≥ pHpzc, the activated carbon surface is charged negatively, so Cd(II) and Co(II) ions and MB molecule which are positively charged, may be easily bound to negatively dissociated forms of the activated carbon groups producing complexes with its surface groups. Although, at pH < pHpzc, the activated carbon surface is positively charged which facilitates the anionic organic compounds and anionic metal ions sorption via interactions adsorbate/adsorbent. Hence, some studies established that the activated carbons with anionic surfactants were negative at all pHs tested because the hydrophilic negatively charged head groups of the surfactants are arranged toward the aqueous phase [45].

5. Conclusion

This study established the feasibility of preparing activated carbons from carob seeds biomass for heavy metal ions removal. The activation was done by HNO_3, which yielded a good quality of activated carbon with high performance for the removal of cadmium and cobalt ions. In this approach, the Box–Behnken experimental design coupled with response surface methodology was used to optimize the preparation conditions of activated carbons for studying the removal of both heavy metal ions. The three most influential factors are investigated including impregnation ratio, activation time and activation temperature in order to study the iodine number, MB index, cobalt and cadmium ions. In the iodine number, the influential factors are the activation time and activation temperature with a negative impact and the impregnation ratio with a positive impact. In the case of the methylene blue index, the influential factors are the impregnation ratio and activation time with a positive impact while the activation temperature has a negative impact. For the elimination of cadmium, the impregnation ratio and the activation temperature with a negative impact, however, the activation time has a positive impact. Hence, for the elimination of cobalt, all factors have a negative impact. For the iodine number, the major value (1,034.83 mg/g) was obtained for a carbon-impregnated with 005 (g/g) and activated at 500°C for 1 h 30 min. For the methylene blue index, the maximum value (279.59 mg/g) was acquired for activated carbon with an impregnation ratio of 0.075 (g/g), during an activation time of 2 h at an activation temperature of 500°C. On the other hand, the carbon activated at 500 °C during 2 h with an impregnation ratio of 0.025 g/g has a higher sorption capacity of cadmium ions. While, in the same conditions but for 1 h, the maximum sorption of cobalt was obtained. Under these optimum preparation conditions and via Langmuir isotherm modeling, the highest sorption capacities were 91.92 mg/g for cadmium and 79.18 mg/g for cobalt ions.

References

[1] M.J. Gonzàlez-Munōz, M.A. Rodriguez, S. Luque, J.R. Álvarez, Recovery of heavy metals from metal industry wastewaters by chemical precipitation and nanofiltration, Desalination, 200 (2006) 742–744.

[2] M. Breida, S.A. Younssi, M. El Rhazi, M. Bouhria, Removal of heavy metals by tight γ-Al_2O_3 ultrafiltration membrane at low pressure, Desal. Water Treat., 167 (2019) 231–244.

[3] R. Kiefer, A.I. Kalinitchev, W.H. Höll, Column performance of ion exchange resins with aminophosphonate functional groups for elimination of heavy metals, React. Funct. Polym., 67 (2007) 1421–1432.

[4] V. Innocenzi, F. Veglio, Separation of manganese, zinc and nickel from leaching solution of nickel-metal hydride spent batteries by solvent extraction, Hydrometallurgy, 129–130 (2012) 50–58.

[5] A.H. Sulaymon, A.O. Sharif, T.K. Al-Shalchi, Removal of cadmium from simulated wastewaters by electrodeposition on stainless steel tubes bundle electrode, Desal. Water Treat., 29 (2011) 218–226.

[6] A. Machrouhi, M. Farnane, A. Elhalil, M. Abdennouri, H. Tounsadi, N. Barka, Heavy metals biosorption by *Thapsia transtagana* stems powder: kinetics, equilibrium and thermodynamics, Moroccan J. Chem., 7 (2019) 98–110.

[7] M. Farnane, A. Machrouhi, A. Elhalil, H. Tounsadi, M. Abdennouri, S. Qourzal, N. Barka, Process optimization of potassium hydroxide activated carbon from carob shell biomass and heavy metals removal ability using Box–Behnken design, Desal. Water Treat., 133 (2018) 153–166.

[8] A. Machrouhi, H. Alilou, M. Farnane, S. El Hamidi, M. Sadiq, M. Abdennouri, H. Tounsadi, N. Barka, Statistical optimization of activated carbon from *Thapsia transtagana* stems and dyes removal efficiency using central composite design, J. Sci.: Adv. Mater. Devices, 4 (2019) 544–553.

[9] S. Hashemian, K. Salari, Z.A. Yazdi, Preparation of activated carbon from agricultural wastes (almond shell and orange peel) for adsorption of 2-pic from aqueous solution, J. Ind. Eng. Chem., 20 (2014) 1892–1900.

[10] P.P. Ndibewu, C.M. Kede, P.G. Tchieta, H.Z. Poumve, A.N. Tchakounte, Simultaneous adsorption of mercury(II) and zinc(II) ions from aqueous solution onto activated carbons derived from a lowland bioresource waste, J. Appl. Surf. Interfaces, 5 (2019) 21–30.

[11] J.B. Mathangi, M.H. Kalavathy, Optimization of process parameters for the adsorption of nickel onto activated carbon using response surface methodology, Desal. Water Treat., 115 (2018) 115–125.

[12] A. El Nemr, A. El-Sikaily, A. Khaled, O. Abdelwahab, Removal of toxic chromium from aqueous solution, wastewater and saline water by marine red alga *Pterocladia capillacea* and its activated carbon, Arabian J. Chem., 8 (2015) 105–117.

[13] H. Tounsadi, A. Khalidi, M. Farnane, A. Machrouhi, A. Elhalil, N. Barka, Adsorptive removal of heavy metals from aqueous solution using chemically activated *Diplotaxis harra* biomass, Surf. Interfaces, 4 (2016) 84–94.

[14] J. Kazmierczak-Razna, B. Gralak-Podemska, P. Nowicki, R. Pietrzak, The use of microwave radiation for obtaining activated carbons from sawdust and their potential application in removal of NO_2 and H_2S, Chem. Eng. J., 269 (2015) 352–358.

[15] S.N. Sun, Q.F. Yu, M. Li, H. Zhao, C.X. Wu, Preparation of coffee-shell activated carbon and its application for water vapor adsorption, Renewable Energy, 142 (2019) 11–19.

[16] S. Mondal, K. Sinha, K. Aikat, G. Halder, Adsorption thermodynamics and kinetics of ranitidine hydrochloride onto superheated steam activated carbon derived from mung bean husk, J. Environ. Chem. Eng., 3 (2015) 187–195.

[17] M. Shoaib, H.M. Al-Swaidan, Optimization and characterization of sliced activated carbon prepared from date palm tree fronds by physical activation, Biomass Bioenergy, 73 (2015) 124–134.

[18] L. Niazi, A. Lashanizadegan, H. Sharififard, Chestnut oak shells activated carbon: preparation, characterization and application for Cr(VI) removal from dilute aqueous solutions, J. Cleaner Prod., 185 (2018) 554–561.

[19] A. Shehzad, M.J.K. Bashir, S. Sethupathi, J.-W. Lim, Simultaneous removal of organic and inorganic pollutants from landfill leachate using sea mango derived activated carbon

via microwave induced activation, Int. J. Chem. Reactor Eng., 14 (2016) 991–1001.

[20] G.-Q. Li, F.-H. Tian, Y.-F. Zhang, J.-L. Ding, Y.-L. Fu, Y. Wang, G.-J. Zhang, Bamboo/lignite-based activated carbons produced by steam activation with and without ammonia for SO_2 adsorption, Carbon, 85 (2015) 448.

[21] L. Lopez, F.C. Janna, S.K. Bhatia, Effect of activating agents: flue gas and CO_2 on the preparation of activated carbon for methane storage, Energy Fuels, 29 (2015) 6296–6305.

[22] S.-A. Sajjadi, A. Meknati, E.C. Lima, G.L. Dotto, D.I. Mendoza-Castillo, I. Anastopoulos, F. Alakhras, E.I. Unuabonah, P. Singh, A. Hosseini-Bandegharaei, A novel route for preparation of chemically activated carbon from pistachio wood for highly efficient Pb(II) sorption, J. Environ. Manage., 236 (2019) 34–44.

[23] T. Mahmood, R. Ali, A. Naeem, M. Hamayun, M. Aslam, Potential of used *Camellia sinensis* leaves as precursor for activated carbon preparation by chemical activation with H_3PO_4; optimization using response surface methodology, Process Saf. Environ. Prot., 109 (2017) 548–563.

[24] N.T. Abdel-Ghani, G.A. El-Chaghaby, M.H. ElGammal, E.-S.A. Rawash, Optimizing the preparation conditions of activated carbons from olive cake using KOH activation, New Carbon Mater., 31 (2016) 492–500.

[25] Y. El Maguana, N. Elhadiri, M. Bouchdoug, M. Benchanaa, Study of the influence of some factors on the preparation of activated carbon from walnut cake using the fractional factorial design, J. Environ. Chem. Eng., 6 (2018) 1093–1099.

[26] M.A. Yahya, Z. Al-Qodah, C.W.Z. Ngah, Agricultural bio-waste materials as potential sustainable precursors used for activated carbon production: a review, Renewable Sustainable Energy Rev., 46 (2015) 218–235.

[27] J. Antony, R.K. Roy, Improving the process quality using statistical design of experiments: a case study, Qual. Assur., 6 (1998) 87–95.

[28] H.P. Boehm, Surface oxides on carbon and their analysis: a critical assessment, Carbon, 40 (2002) 145–149.

[29] J.S. Noh, J.A. Schwarz, Estimation of the point of zero charge of simple oxides by mass titration, J. Colloid Interface Sci., 130 (1989) 157–164.

[30] S. Das, S. Mishra, Box–Behnken statistical design to optimize preparation of activated carbon from *Limonia acidissima* shell with desirability approach, J. Environ. Chem. Eng., 5 (2017) 588–600.

[31] Y.H. Li, Q.J. Du, X.D. Wang, P. Zhang, D.C. Wang, Z.H. Wang, Y.Z. Xia, Removal of lead from aqueous solution by activated carbon prepared from *Enteromorpha prolifera* by zinc chloride activation, J. Hazard. Mater., 183 (2010) 583–589.

[32] I. Langmuir, The constitution and fundamental properties of solids and liquids. Part I. Solids, J. Am. Chem. Soc. 38 (1916) 2221–2295.

[33] H. Freundlich, W. Heller, The adsorption of *cis-* and *trans-*azobenzene, J. Am. Chem. Soc., 61 (1939) 2228–2230.

[34] A. Ebrahimi, M. Ehteshami, B. Dahrazma, Isotherm and kinetic studies for the biosorption of cadmium from aqueous solution by *Alhaji maurorum* seed, Process Saf. Environ. Prot., 98 (2015) 374–382.

[35] D. Mohan, K.P. Singh, Single- and multi-component adsorption of cadmium and zinc using activated carbon derived from bagasse—an agricultural waste, Water Res., 36 (2002) 2304–2318.

[36] Z.Z. Guo, J.L. Fan, J. Zhang, Y. Kang, H. Liu, L. Jiang, C.L. Zhang, Sorption heavy metal ions by activated carbons with well-developed microporosity and amino groups derived from *Phragmites australis* by ammonium phosphates activation, J. Taiwan Inst. Chem. Eng., 58 (2016) 290–296.

[37] P.D. Meshram, S.S. Bhagwat, Removal of Cd(II) Ions from Aqueous Solution by Adsorption on $ZnCl_2$-Activated Carbon: Equilibrium and Kinetic Study, I. Regupathi, K. Vidya Shetty, M. Thanabalan, Eds., Recent Advances in Chemical Engineering, Springer, Singapore, 2016.

[38] H. Kasaini, P.T. Kekana, A.A. Saghti, K. Bolton, Adsorption characteristics of cobalt and nickel on oxalate-treated activated carbons in sulfate media, World Academy of Science, Eng. Technol., 76 (2013) 707–721.

[39] R. Prabakaran, S. Arivoli, Removal of cobalt(II) from aqueous solutions by adsorption on low cost activated carbon, Int. J. Sci. Eng. Technol. Res., 2 (2013) 271–283.

[40] H. Tounsadi, A. Khalidi, M. Farnane, M. Abdennouri, N. Barka, Experimental design for the optimization of preparation conditions of highly efficient activated carbon from *Glebionis coronaria* L. and heavy metals removal ability, Process Saf. Environ. Prot., 102 (2016) 710–723.

[41] H. Tounsadi, A. Khalidi, A. Machrouhi, M. Farnane, R. Elmoubarki, A. Elhalil, M. Sadiq, N. Barka, Highly efficient activated carbon from *Glebionis coronaria* L. biomass: optimization of preparation conditions and heavy metals removal using experimental design approach, J. Environ. Chem. Eng., 4 (2016) 4549–4564.

[42] Y.P. Guo, D.A. Rockstraw, Physical and chemical properties of carbons synthesized from xylan, cellulose, and kraft lignin by H_3PO_4 activation, Carbon, 44 (2006) 1464–1475.

[43] M. Jagtoyen, F. Derbyshire, Some considerations of the origins of porosity in carbons from chemically activated wood, Carbon, 31 (1993) 1185–1192.

[44] S. Sato, K. Yoshihara, K. Moriyama, M. Machida, H. Tatsumoto, Influence of activated carbon surface acidity on adsorption of heavy metal ions and aromatics from aqueous solution, Appl. Surf. Sci., 253 (2007) 8554–8559.

[45] C. Akmil Başar, A. Karagunduz, B. Keskinler, A. Cakici, Effect of presence of ions on surface characteristics of surfactant modified powdered activated carbon (PAC), Appl. Surf. Sci., 218 (2003) 170–175.